

An Approach to Studying the Impact of Bird Strike in Jet Engine Blade at High Altitude Considering the Effect of Cumulative Stress

Vrugisha Thakkar¹, Datt Patel²

¹A. D. Patel Institute of Technology, ²R. N. G. Patel Institute of Technology

Submitted: 01-04-2021

Revised: 11-04-2021

Accepted: 14-04-2021

ABSTRACT: High stresses during flight induced in the jet engine blade are considerable threats to flight safety and have resulted in several human injuries accidents. The factors that can cause blade damaging are bird strikes, fatigue, creeping, stagnant pressure and centrifugal force, etc. The literature shows that centrifugal forces increase stress in the root section during the flight. Bird strikes will have an important effect on blade damage in this situation. The present paper examined a simulation with a bird strike speed of 89.611 m/s (174.18 knots) of jet engine blades at 810 rad/sec (7,734 rpm). Initially, single blade simulation by the fluid structural interaction was performed using pressure and stress distribution at high altitude. Effective stress vs. time chart was drawn to understand the physical phenomenon by the simulation to prevent accidents by requiring modification in the design of a single blade.

Keywords: Bird-strike, Centrifugal stress, CE/SE solver, LS-DYNA, Pressure distribution.

I. INTRODUCTION

Due to centrifugal force and airflow pressure during normal flight conditions, jet engine blades are subjected to stress. The jet engine blades are subject to high temperature, high stresses and a potentially high vibration environment. All three can cause blade failure and can cause the engine to fail as indicated[1]. The blade induces intense stress in case of a bird strike. From 1990 to 2008, almost ninety thousand birds hit the commercial aeroplane, which resulted in immense monetary losses due to repair, delay and cancellation, was reported to the US Federal Aviation Administration (FAA) alone in the USA[2]. Costs from 614 to 1.28 billion US\$ per year as indicated in the report[3].

Many researchers have submitted an independent simulation of the stress of centrifugal forces, airflow and bird strike in a blade[4, 5]. In

this project, the cumulative effect of the loads on the blade was investigated. Multidisciplinary simulation in complex domains using advanced techniques was a problem. The LS-DYNA software adapted and adapted a detailed finite element model of the Jet Engine Turbine. The CE/SE solver initially gives the pressure through simulation of the airflow on the blades. The solver is a preservative element. The distribution of pressure was found to be in good harmony with literature results [6], as shown in figure 4. (a). As a result of rotation (810 rad/sec), the centrifugal force was induced in the blades. At the same time an external object such as a bird drawn in the engine by the airflow damages the blade, the external case and other elements.

A bird model has been developed and validated based on available literature experimental results. The bird is produced by SPH (Smoothed Particle Hydrodynamics) method. At a speed of 174.18 knots (89.611 m/s), it was made for an impact on the blades. The result shows the cumulative effect, which is useful in design and optimization, of various types of loads on the engine blades.

Although much in-house bird strike, centrifugal force effect, blade life cycle experiment has been carried out by aerospace organisations on a ground level, it is difficult to conduct these experiments for real flight conditions. This paper focuses on determining combined strains on the blades, where the engine is kept in real-time conditions artificially created.

II. METHODOLOGY

In the simulation of jet blades for bird strikes, the following assumptions are considered:

1. The blade's angular velocity is 810 rad/sec, and the material is homogeneous.
2. The weight of the bird is 4 pounds (1.8 kilograms)[7]

3. The bird's impact velocity on the blades was 174.18 knots (89.611 m/s).
4. The air's velocity is constant over a given altitude range.

1. Phases of flight

LS DYNA is used to simulate three phases of flight: take-off, climb, and cruise at different altitudes, along with other input conditions such as

pressure, temperature, density, and air velocity. The various phases of flight are as follows:
 Take-off/Landing Velocity: - (120-150) Knots
 Climb velocity: - (280-310) Knots
 Cruise Velocity: - (240-250) Knots
 Stagnation pressure acting on fluid, Von-misses stress, and external pressure acting on the blade are output measures.

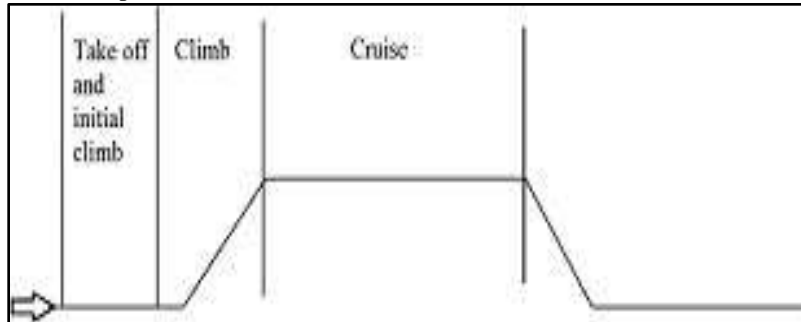


Figure 1 Flight's phases

2. Material and dimensions of the blade

Because of the unique combination of mechanical, corrosion and physical characteristics, titanium fan blades have historically shown good efficiency. Titanium has excellent tensile strength and a strong output, a low life cycle cost, is available easily and results in the highest strength to weight ratio compared to other structural metals in combination with its low density. Titanium costs, which were initially higher, can be multiplied by economies resulting from long component life and the corresponding reduction in the maintenance and downtime of aircraft. In addition, titanium creates an oxide on the blade surface that can

withstand interactions with other atmospheric elements[9, 10].

T. Miyachi discussed the use of polymer matrix composite materials to fan blades to reduce the weight of high turbofan engines in a highly effective manner. The weight of fans with composite materials such as Ti 6Al- 4V was reduced by 30% or more[11]. As in Table-1, which was considered by simulation, the material characteristics are shown.

Figure 2 shows the structure of a single blade with Table-2 dimensions. For simulation, the developed single blade model has been used. The blade model was taken from the LSTC aerospace group.

Table 1 Material Property

Parameter	Notation	Ti 6Al- 4V	SI Unit
Density	ρ	0.160043 (lb./in ³)	4429.97 (Kg/m ³)
Poisson ratio	ν	0.33	
Modulus of elasticity	E	1.6E+7 (psi)	1.1E+11 (N/m ²)
Static yield limit	A	159,246 (psi)	1.09E+9 (N/m ²)
Strain hardening modulus	B	158,376	

Table 2 Blade Feature

Component	Measures	SI Units
Blade-tip radius	20 in	0.508 m
Blade-root radius	6 in	0.152 m
Blade-root area	0.9 in. ²	0.0005 m ²
Blade-root stagger angle	17°	-
Blade-tip stagger angle	40°	-
Blade chord at the tip	5.2 in	0.132 m
Blade chord at the root	4.5 in	0.114 m

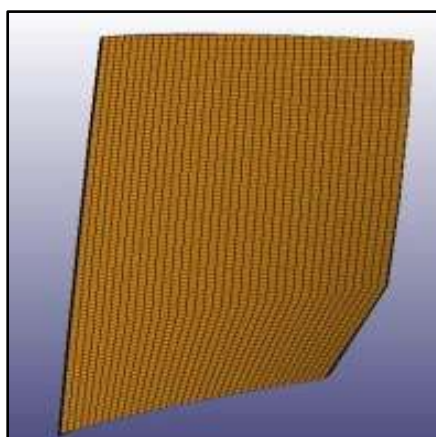


Figure 2 Structure of blade

3. Pressure and stress distribution because of airflow in a blade

At different atmospheric conditions, the pressure on the blades differs due to airflow. The compressible fluid solver is used in LS-DYNA in this varying condition[12]. As shown in Figure 3, the blade is kept in a rectangular box. Table 3 and 4

specify the airflow behaviours and CESE solver parameters[13].

CESE_EOS_IDEAL_GAS define the coefficients C_v and C_p in the equation of state for an ideal gas in CESE fluid solver. CESE_MAT_001 (GAS) defines the fluid (gas) properties in a viscous flow for the CESE solver[14].

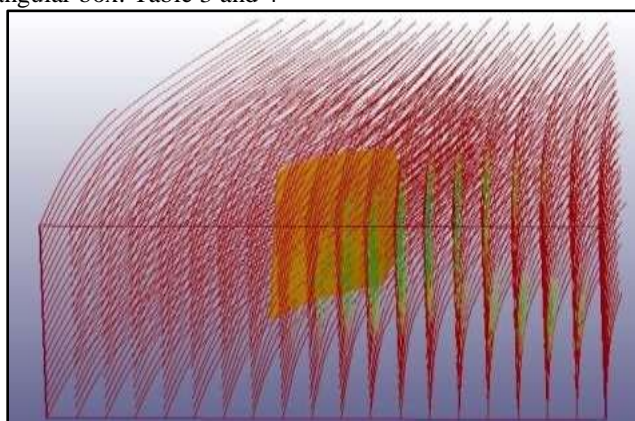


Figure 3 Streamline of air impacting on the blade

Table 3 Different keywords used in CESE solver

Sr. No.	Keywords	Purpose
1	CESE_BOUNDARY_NON_REFLECTIVE	To develop a non-disturbed uniform flow for a specified boundary at entry (Input) level.
2	CESE_EOS_IDEAL_GAS	To define coefficients C_v and C_p in the equation of state for an ideal gas.
3	CESE_MAT_001 (GAS)	To define the fluid (gas) properties.

Table 4 Data of air properties at different altitude

Sr. No.	Altitude (ft.)	Velocity (v) of air	Pressure of air(psi)
1	30-900	65m/s	14.679
2	1000-9000	108m/s	13.669
3	Above 10,000	150 m/s	10.669

The International Atmosphere Standard gives the value of air density and pressure[8]. By the following Bernoulli equation, the value of air velocity can be calculated.

$$P = \frac{1}{2} \rho v_a^2$$

Where, P = Pressure of Air, ρ = Density and v_a = Air Velocity

The values of pressure and stress are listed in Table 5 for different altitude conditions.

The trend is achieved by neglecting the effect of bird strikes and centrifugal force at various altitudes in the stationary blade. The trend of stress and pressure is observed to dwindle as the altitude increases.

Table 5 Maximum pressure & stress at different altitude

Sr. No.	Altitude (ft.)	Max. Pressure(psi)	Max. Stress(psi)
1	30-900ft	23.186	27.3096
2	1000-9000 ft.	21.5759	25.4097
3	Above 10,000 ft.	15.9422	18.7717

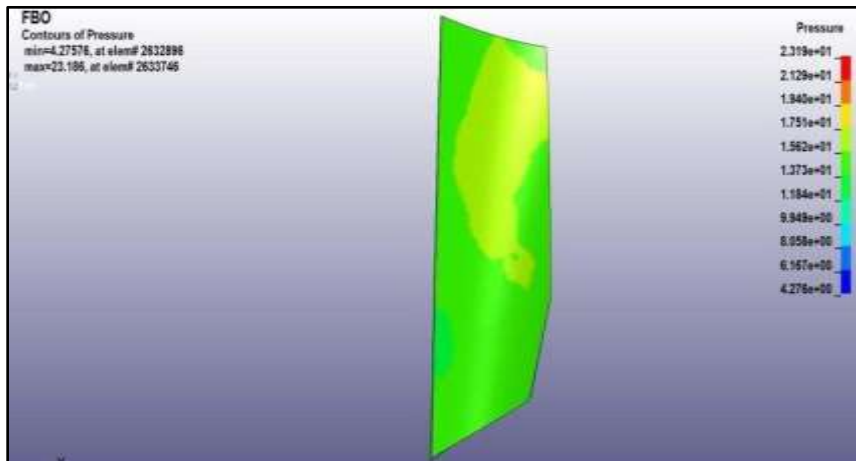


Figure 4 Pressure on the blade, when a fluid strike on the blade

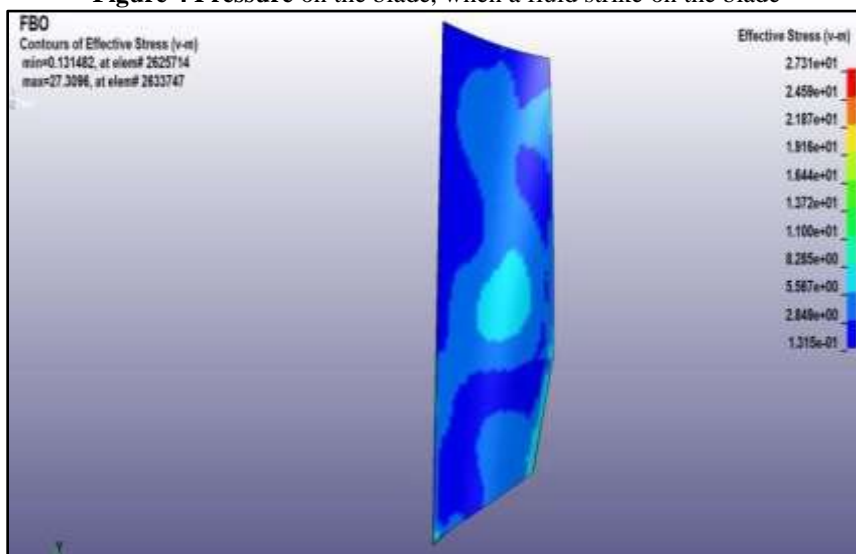


Figure 5 Stress on the blade, when a fluid strike on the blade

4. Centrifugal stress generated inblade

The blades as shown in Figure 6 rotate at 816 rad/second angular velocity. The part id of the blades is assigned by VELOCITY GENERATION. In the particular elements of the blade, where the bird may crash with the blade, stress was induced by approximately 101827psi [702.07 MPa]. The average blade stress is 6,110E+04psi[421Mpa], as shown in Figure 6. As shown in Figure 7 The stress near the hub is greater than the tip section.

Effective stress Vs time graph of different nodes near bird strike locations is plotted as shown in figure 8.

The centrifugal force in a high-speed rotating blade cannot be ignored since the fan rotation is more than fifty thousand times as high as the centrifugal acceleration. This increases the resistance to impacts and reduces the deformation of the blade[5].

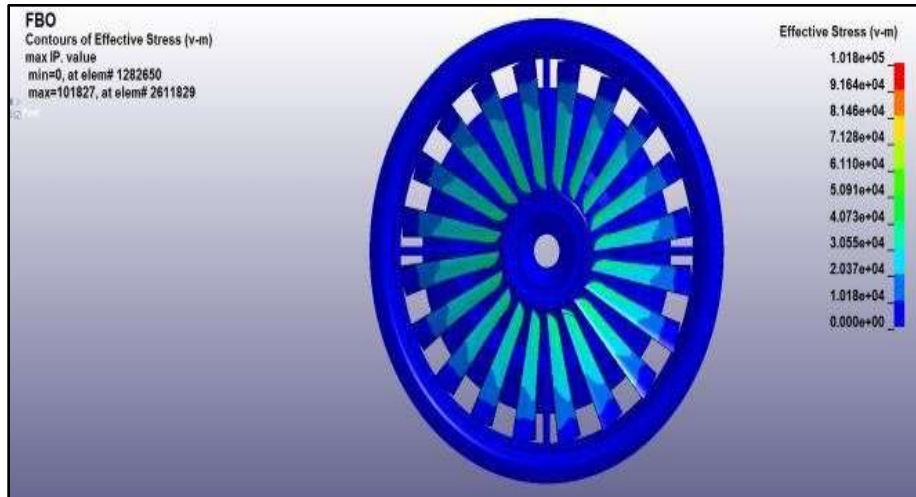


Figure 6 Variation of stress from hub to tip of the blade

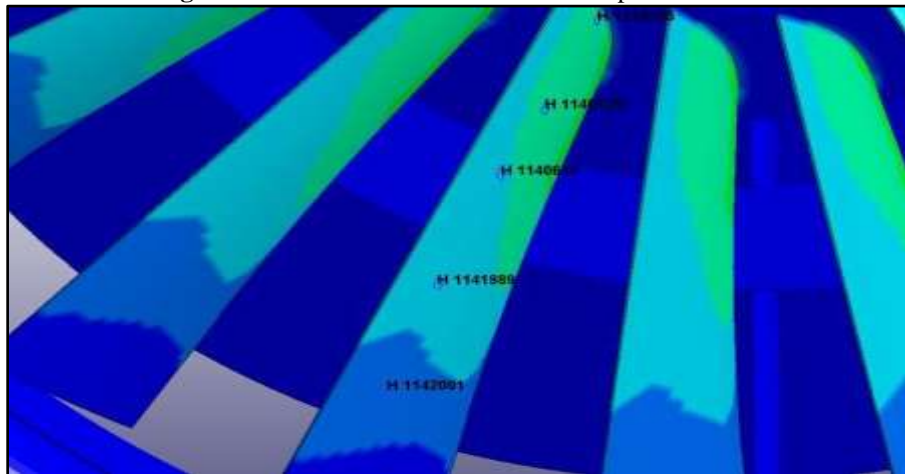


Figure 7 Variation of stress from hub to tip of the blade

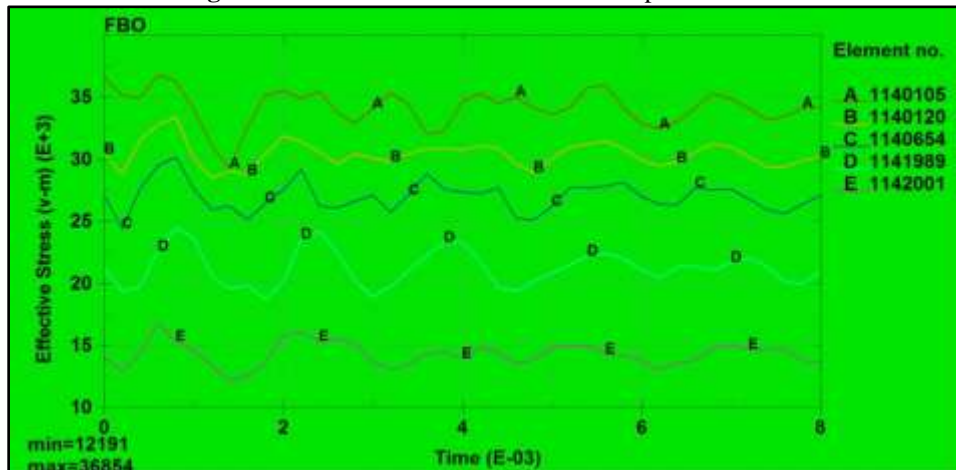


Figure 8 stress v/s time

5. Stress in a blade due to birdstrike

On the solid single blade, a separate bird strike test is done. The first step in Astrophysics was to deal with fluid masses that are moved arbitrarily in tri-dimensional space. The Smoothed

Hydrodynamics Particles was introduced. Because the SPH method is purely Lagrangian, finite element solutions based on a Lagrangian formulation can be linked easily. Furthermore, the SPH technology may handle problems involving

large deformations more easily due to the lack of a mesh connecting each particle. The continuum is treated as a random number of interacting particles in the SPH method. SPH is a technique with the basis of interpolation theory, which allows all functional values of the same function to be expressed in a set of disordered points that make up the continuum. In the absence of regular connectivity between particles found in mesh processes, Spatial derivatives of several field variables are calculated using kernel estimates[15]. A sphere with a density of 950 kg/m³ is considered the form of the bird.

The projectile response to the impact can be divided, according to Martin NF, into five categories, depending on the speed of impact: elastic, plastic, hydrodynamic, sonic or explosive. The internal stresses in the projectile fall under the material strength during an elastic impact so that it recovers. The plastic response of the impactor begins with increased impact speed, but the material strength remains adequate to prevent a fluid-like behaviour. An additional increase in impact speed leads to inner stress exceeding the strength and liquid flow of the projectile. The material density determines the reaction of the impactor at this impact velocity. In this case, material strength is not going to play a role. Typically this flow behaviour can be observed in high-speed impact test films.

The bird impactor is therefore treated with the speeds of interest as a so-called "soft body," since the stresses in the bird are far superior to their strength in themselves. During impact, the load extends over a relatively large area[16]. During flight collisions between motors and birds are classified as events of soft impact. The effect is soft when the projectile is much less strong than the target and causes large-scale projectile distortions across the target surface[17, 18].

To define the bird's behaviour, a fluid material model was used in conjunction with a pressure-volume State Equation (EOS). In this combined model the bird mass was defined and the volume changes in SPH particles were associated with the hydrostatic pressure on the particle while ignoring the deviatoric stresses caused by shear stiffness[19].

The distribution of stress due to bird strike and effective stress vs time is shown respectively in Figures 9 and 10. From the simulation carried out, it was noted that only bird striking considerations were effective stress on the blade at 44778 psi (308.73 MPa). Other references validate the results extensively. The bird is beginning to affect the middle portion of Blade. In the contact area, the maximum equivalent stress is 265 MPa[20].

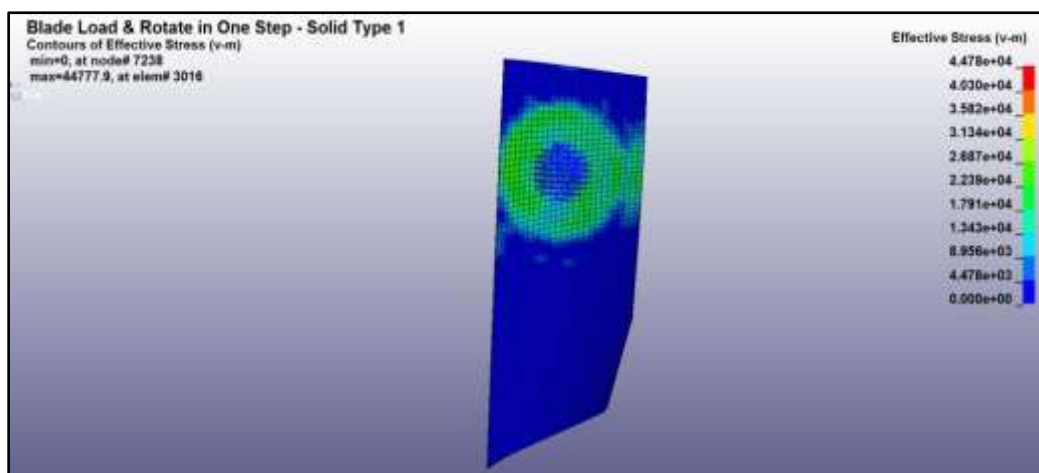


Figure 9 Stress generated on the blade at a time of bird-strike

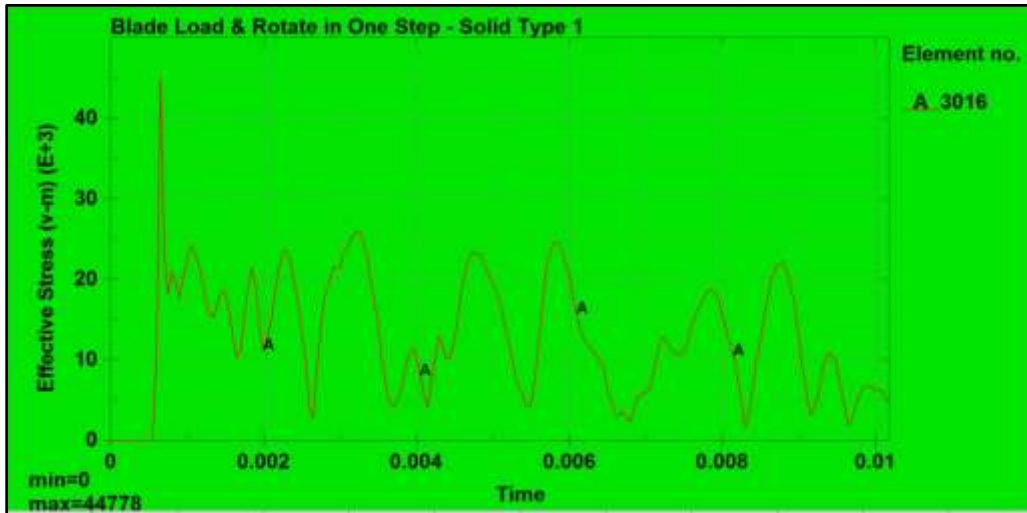


Figure 10 stress v/s time

6. Cumulative stress determination in ablade

Combined stress is also investigated, considering the preceding conditions to imitate the real flight scenario. The angular velocity is 810 rad/sec to determine pressure due to centrifugal force.

Two posts: Multifunction post and basic post. LS-Dyna is made of two posts. The Multi-solver post provides fluid dynamic results whereas the base after results are related to the structure of

the solid/shell. But in the basic post result of a bird strike that can be utilised by a multi-post solver, fluid streamlines are not generated.

The pressure of the fluid is shown in Figure 11. When it strikes the blade, the pressure decreases from 1.944E+01psi to 1.758E+01ppi. [The multi-solver post allows the interaction structure not to be visible, but considers the interaction effect]. The pressure value on the edges of the blades is shown in Figure 12.

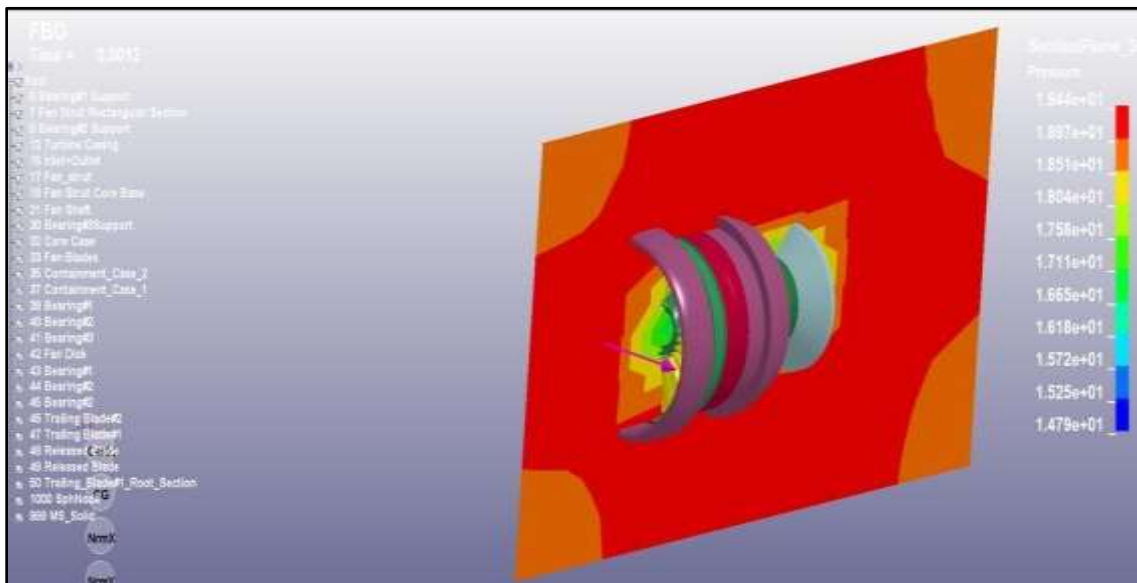


Figure 11 Pressure of the fluid, When striking on the rotating blade

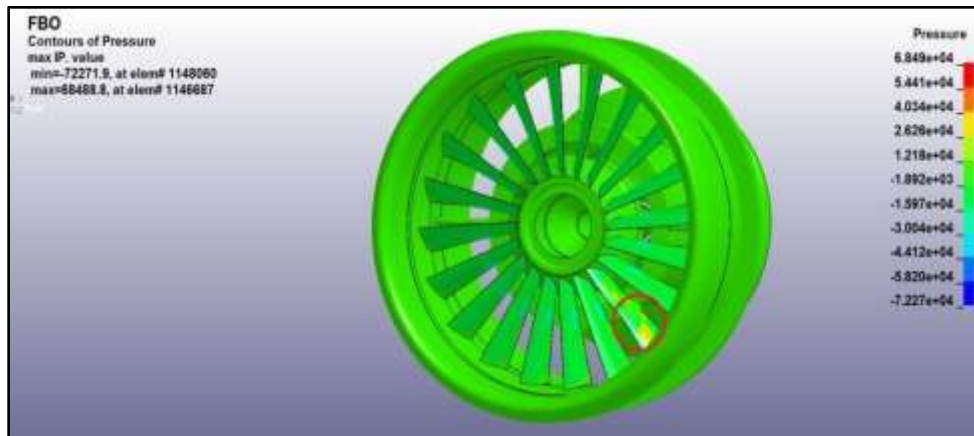


Figure 12 Pressure promoted on the blade due to bird strike

At the moment of the bird strike in a target blade, air pressure generated by the motor reaches about $1.218E+04$ psi. Stiffness was defined for minimising simulation time for other components such as the case and shaft. There is therefore no stress on them. All conditions mentioned above cause stress variation in the blades. The results

above show the stress alloy of the blade from 30 to 900 metres above sea level. At the root of the strike and the area where the impact occurred, a lot of stress was generated. Specific elements have therefore been selected and the graph is drawn as shown in Fig.15.

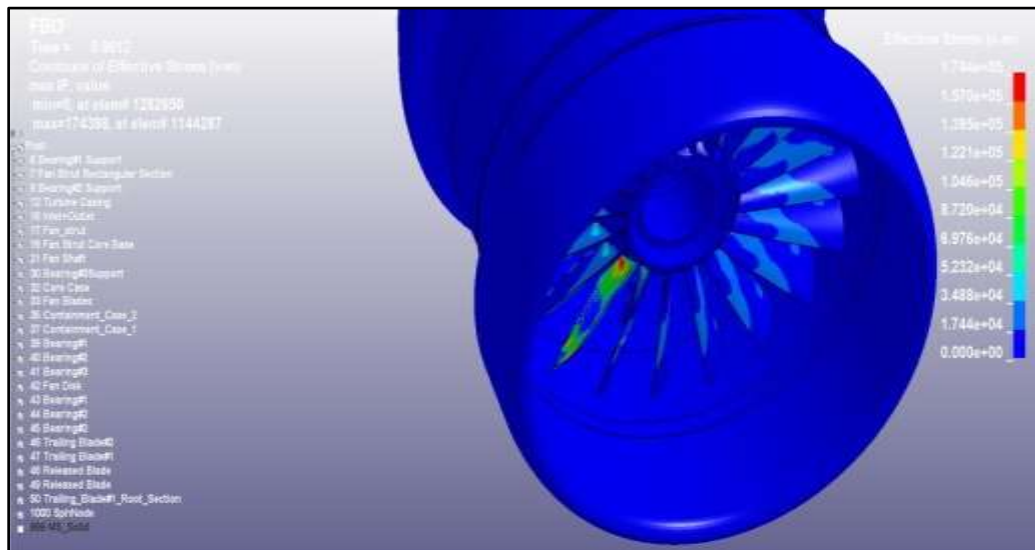


Figure 13 High stresses are promoted in the blade due to bird strike

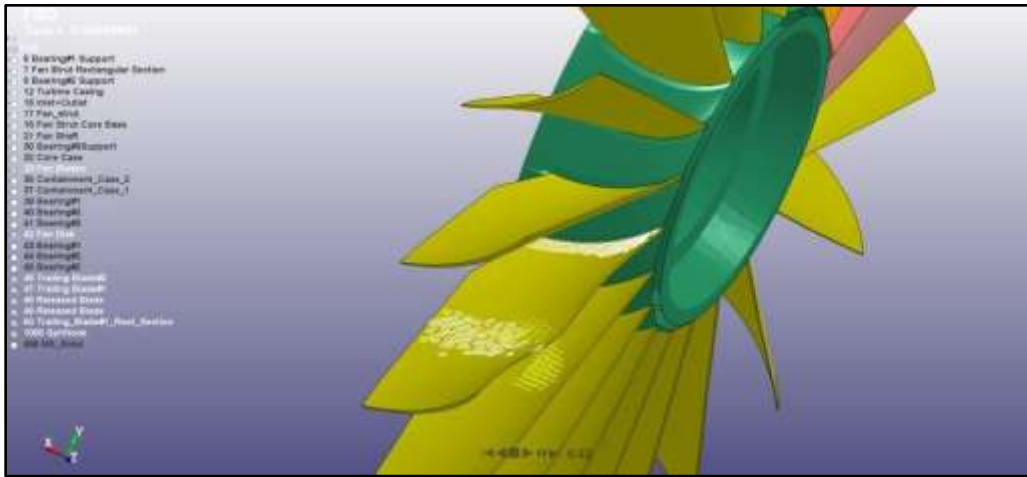


Figure 14 Selected element of the targeted blade

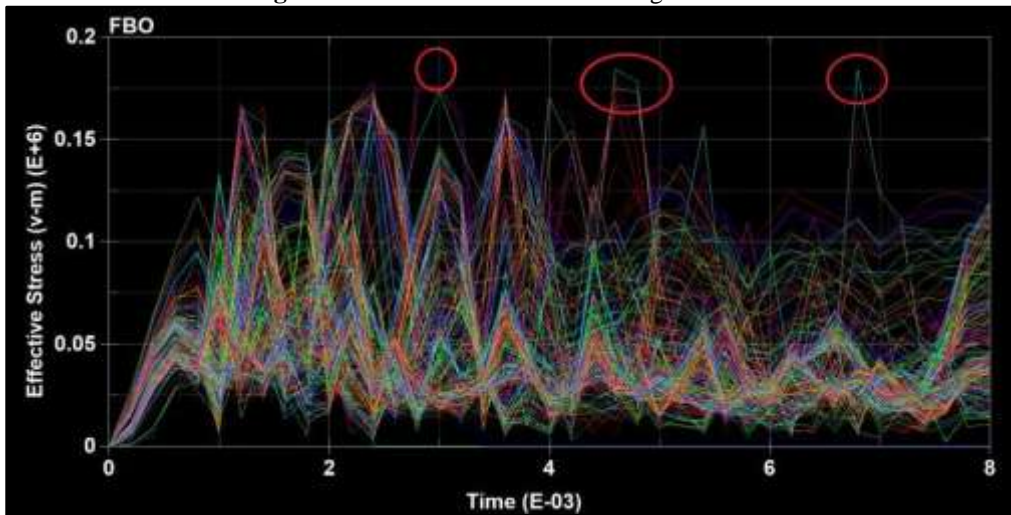


Figure 15 Stress V/s Time

During a bird strike, some of the elements experienced high-stress patterns as a result of bending causes after effects, which are about 174389 psi [1202,36 MPa] stress-induced. In

general, 1202.36 MPa has been stressed during the event in blades. The results for various altitudes as set out in Table 6 are also obtained.

Table 6 Von-Mises stresses induced in the blade at different altitude

Sr. No.	Altitude Range	Von-Mises Stress
1	30 – 900 ft.	174389 psi (1202.36 MPa)
2	1000 – 9000 ft.	173790 psi (1198.23 MPa)
3	Above 10,000 ft.	173477 psi (1196.08 MPa)

III. RESULT AND DISCUSSION

There are stresses near each other at three different levels (Table. 6). Because the relative velocity at 65m/s at 30-900 ft. is low, the fluid density is high and the density increases, the stress and the other way around [21]. At 150m/s, the relative velocity is high at an altitude above 10,000 ft but the fluid density is low. This is why in each phase of flight, stress is induced nearby.

IV. CONCLUSION

With the help of “LS-Dyna” software, various stresses on the jet engine blade at different altitudes are achieved successfully. LS-Dyna is an ideal tool for high-speed impact situation with its powerful damage and failure modelling capabilities for the transient dynamic analysis of highly non-linear issues. Before actual testing, a large amount

of money can be saved by numerical simulations. The numerical simulation provides more than experimental results and can be used to check and supplement experimental results. The cumulative stress effect results in a simulation, which means that the airflow stress is much smaller than the effect and centrifugal stress. The impact on the tip of the blades of the bird is greater than in the centre of the blades. At different altitudes, the stresses generated do not change drastically because increases in relative speed are reduced by density at higher altitudes. The impact resistance of blades is increased by centrifugal force and stress is generated below the yield strength of the blade material which indicates that the design is safe and does not cause blade failure.

REFERENCE

- [1] Bhagi, L K Gupta, Pardeep and Vikas Rastogi "A Brief Review on Failure of Turbine Blades" STME- 2013, Smart Technologies for Mechanical Engineering 25-26 Oct 2013 at Delhi Technological University, Delhi.
- [2] Dolbeer RA, Wright SE, Weller J, Begier MJ. "Wildlife strikes to civil aircraft in The United States 1990– 2008". FAA National Wildlife Strike Database, Serial Report Number 15, September, 2009.
- [3] Allan JR, Orosz AP. "The costs of bird strikes to commercial aviation". In Proceedings of the 2001 bird strike committee-USA/Canada 3rd joint annual meeting, Calgary, Canada; 2001p.218-226
- [4] Aaron J. Siddens and Javid Bayandor "Crashworthiness for Aerospace Structures and Hybrids (CRASH)," Computer and Structures Vol.122, June 2013,p.178-191.
- [5] Miyachi, T., Okumura, H., and Ohtake, K., "An Analysis of the Effect of Centrifugal Force on the Impact Resistance of Composite Fan Blades for Turbo-Fan Engines," SAE Technical Paper 912047, 1991p.246- 253
- [6] Karna S. Patel, Saumil B. Patel, Utsav B. Patel, Pr of. Ankit P. Ahuja., "CFD Analysis of fan Aerofoil", International Journal of Engineering Research Vol.3, March 2014, p. 154-158.
- [7] Chuan KC (2006) Finite element analysis of bird strikes on composite and glass panels. PhD dissertation, BSc thesis, National University of Singapore.
- [8] Standard Atmospheric Pressure at Different Altitudes.
- [9] Phases of flight-<https://www.fp7-restarts.eu>
- [10] Leye M. Amoo., "On the design and structural analysis of jet engine fan blade structures", Progress in Aerospace Sciences, Volume 60, 2013 p.1-11.
- [11] T. Miyachi, "Research on the Application of Composites for High Bypass Ratio Turbo-Fan Engines", Proceedings of the 29th Conference on Aircraft Engines, Feb. 1989, p.20-25.
- [12] LS-DYNA Aerospace Working Group.
- [13] LSTC-Manual Theory –II MULTI-PHYSICS-SOLVER.
- [14] LSTC-Manual Theory –II Material Models.
- [15] Nizampanam, L. S., "Models and Methods for Bird Strike Load Predictions", PhD thesis, Wichita State University, 2007.
- [16] Martin NF. "Nonlinear finite-element analysis to predict fan-blade damage due to soft-body impact". J Propul Power 1990, p.445–50.
- [17] Kim, M., Zammit, A. and Bayandor, J. "Bird Strike Damage Tolerance Analysis of Composite Turbofan Engines," 27th Congress of the International Council of the Aeronautical Sciences, Proceedings of ICAS 2010, Nice, France, 2010, p.19-24.
- [18] Wilbeck, J.S. "Development of a Substitute Bird Model," Journal of engineering for power Vol. 103, No. 4, 1981, pp. 725-730.
- [19] Jenq, S. T., Hsiao, F. B., Lin, I. C., Zimcik, D. G. and Ensan, M. N. "Simulation of a rigid plate hit by a cylindrical hemi-spherical tip-ended soft impactor," Computational Materials Science Vol. 39, 2007.
- [20] Guan Yupu, Zhao Zhenhua, Chen Wei, Gao Deping. "Foreign object damage to fan rotor blades of aero engine part ii: numerical simulation of bird impact", Chinese journal of Aeronautics, Vol 21, Issue 4, August 2008, p. 328-334
- [21] N.A. Fleck and R.A. Smith, "Effect of density on tensile strength, fracture, toughness, and fatigue crack propagation behavior of sintered steel", Taylor & Francis Vol 24, 1981, p.121-125.



**International Journal of Advances in
Engineering and Management**
ISSN: 2395-5252



IJAEM

Volume: 03

Issue: 04

DOI: 10.35629/5252

www.ijaem.net

Email id: ijaem.paper@gmail.com